OMTM, Volume *21*

Supplemental information

Voluntary wheel running complements microdystrophin gene therapy to improve muscle function in mdx mice

Shelby E. Hamm, Daniel D. Fathalikhani, Katherine E. Bukovec, Adele K. Addington, Haiyan Zhang, Justin B. Perry, Ryan P. McMillan, Michael W. Lawlor, Mariah J. Prom, Mark A. Vanden Avond, Suresh N. Kumar, Kirsten E. Coleman, J.B. Dupont, David L. Mack, David A. Brown, Carl A. Morris, J. Patrick Gonzalez, and Robert W. Grange

Supplemental Figures

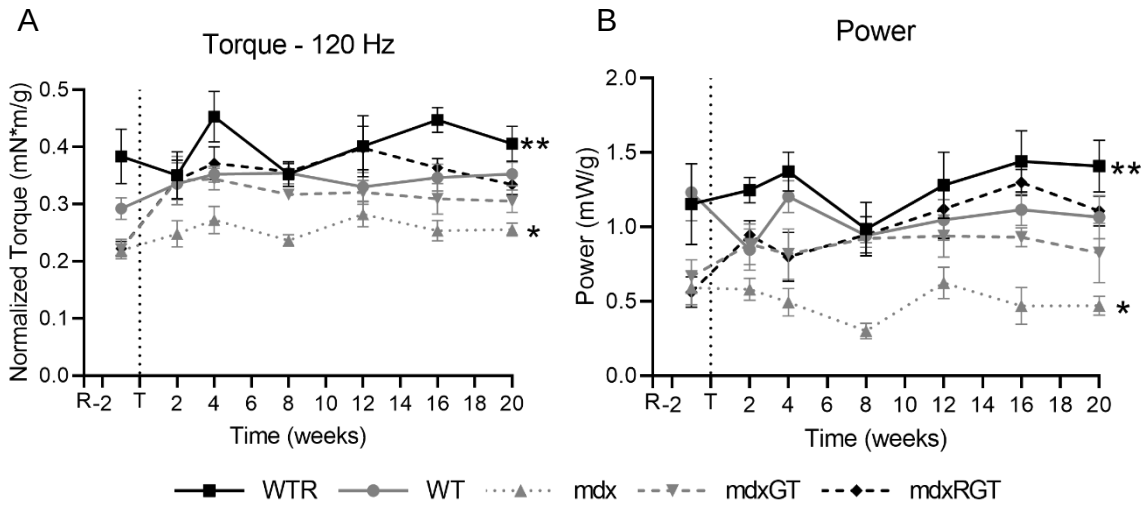

Figure S1. (A) In vivo plantarflexor torque at 120Hz over time. *mdx < all groups at all time points post-treatment; **WTR > WT, mdxGT at all time points post-treatment. **(B)** Peak power over time, *mdx < all groups; **WTR > all groups at all time points post-treatment. Mean ± SE. All comparisons $p<0.05$. WTR, n=7; WT, n=8; mdx, n=7; mdxGT, n=8; mdxRGT, n=8.

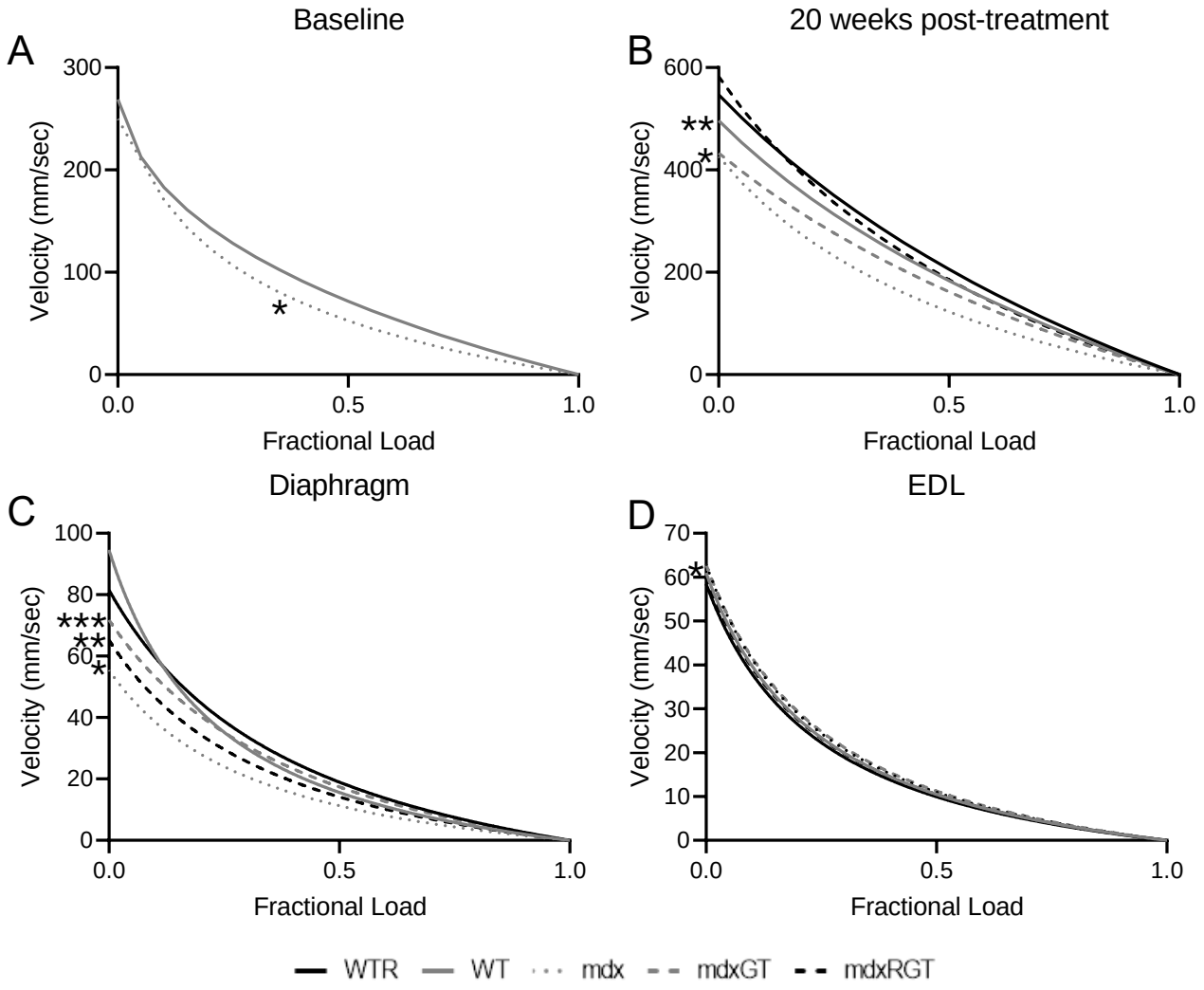

Figure S2. Representative torque- and force-velocity curves. In vivo plantar flexor torque-velocity at baseline and 20 weeks post-treatment **(A, B).** Ex vivo force-velocity in diaphragm and EDL muscles **(C, D)**. **(A)** ***mdx < WT. **(B)** ***mdx, mdxGT < WT, WTR, mdxRGT; **WT< WTR. **(C)** *mdx<all groups; **mdxRGT< WT, WTR, mdxGT; ***mdxGT<WTR. **(D)** *WTR < WT, mdx, mdxGT; mdxRGT< mdx, mdxGT; WT< mdxGT. Curve comparisons $p<0.05$. WTR, n=5; WT, n=7; mdx, n=5; mdxGT, n=7; mdxRGT, n=6.

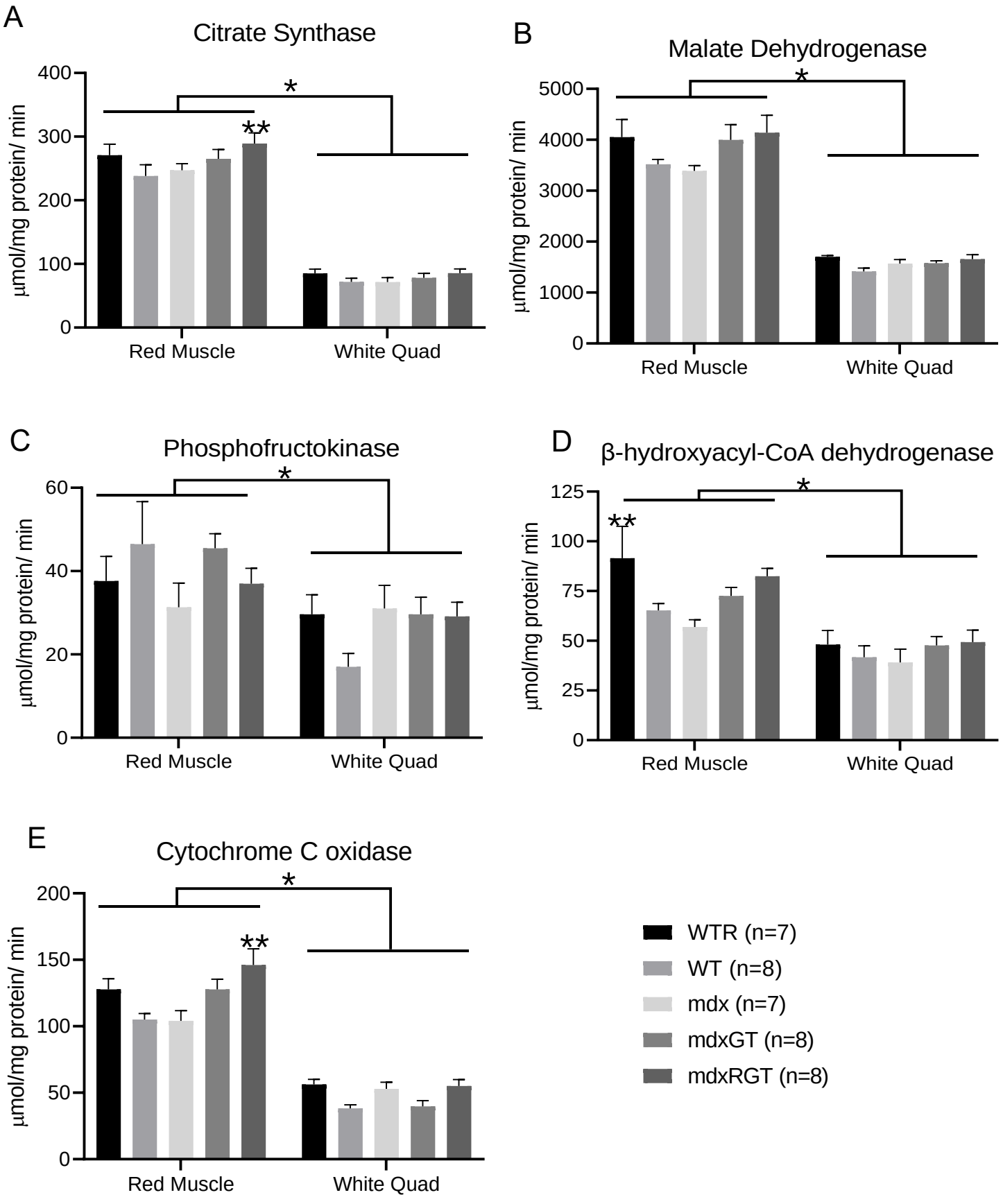
A
Citrate Synthase
µmol/mg protein/ min
400
300
200
100
0
*
**
Red Muscle
White Quad
B
Malate Dehydrogenase
µmol/mg protein/ min
5000
4000
3000
2000
1000
0
*
Red Muscle
White Quad
C
Phosphofructokinase
µmol/mg protein/ min
60
40
20
0
*
Red Muscle
White Quad
D
β-hydroxyacyl-CoA dehydrogenase
µmol/mg protein/ min
125
100
75
50
25
0
*
**
Red Muscle
White Quad
E
Cytochrome C oxidase
µmol/mg protein/ min
200
150
100
50
0
*
**
Red Muscle
White Quad
WTR (n=7)
WT (n=8)
mdx (n=7)
mdxGT (n=8)
mdxRGT (n=8)

Figure S3. Metabolic enzyme activity assays in soleus combined with red gastrocnemius (Red Muscle), and white quadriceps (White Quad). (A) Citrate synthase activity, *Red > white**, ****mdxRGT > WT**. **(B)** Malate dehydrogenase activity, *Red > white. **(C)** Phosphofructokinase activity, *Red > white. **(D)** BHAD activity, *Red > white; **WTR > mdx. **(E)** Cytochrome C oxidase activity, *Red > white; **mdxRGT > WT, mdx. All comparisons $p<0.05$.

A

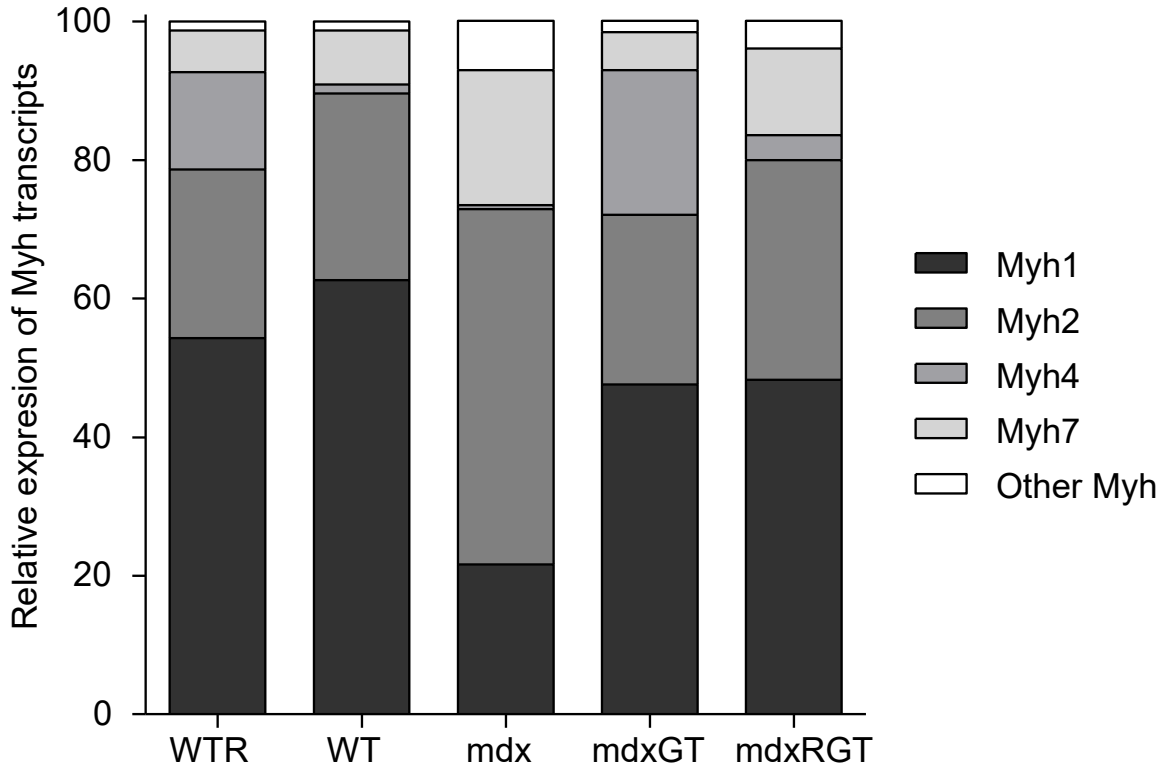

B

	WTR	WT	mdx	mdxGT	mdxRGT
Myh1 (IIx)	54.3	62.7	21.6	47.6	48.3
Myh2 (IIa)	24.3	26.9	51.3	24.5	31.7
Myh4 (IIb)	14.1	1.3	0.59	20.9	3.6
Myh7 (I)	6.0	7.8	19.5	5.5	12.5
Other Myh	1.3	1.3	7.1	1.6	4.0
TOTAL	100	100	100	100	100

Figure S4. (A) Myosin heavy chain (Myh) transcript distribution. Relative to WT or WTR, mdx has low IIx and little IIb expression, and increased myosin type IIa and I expression. This myosin distribution supports low power output (Fig. 7B). Microdystrophin gene therapy alone improves the myosin type distribution to support increased power. Running combined with microdystrophin gene therapy in the mdxRGT diaphragm promotes a slower phenotype vs mdxGT. In mdxRGT, myosin type IIx is unchanged, I and IIa are increased and IIb is decreased vs mdxGT. This shift in myosin transcript distribution if matched by myosin heavy chain content supports the decrease in diaphragm power of mdxRGT (Fig. 7B). Note: mdxGT has a greater proportion of myosin IIb vs mdxRGT which tracks with increased power (Fig. 7B). **(B)** Relative expression of Myh transcripts in the different groups (corresponding fiber type for Myh). Mdx gene expression data matches closely with mdx diaphragm fiber type.[4] In%, Burns (herein): Type I, ~10(I, 20); IIA, 57(IIa, 51); IIX, 25(IIx, 22); IIB, 1(IIb, 0.6); Other, 7(7). WTR, n=7; WT, n=8; mdx, n=7; mdxGT, n=8; mdxRGT, n=8.

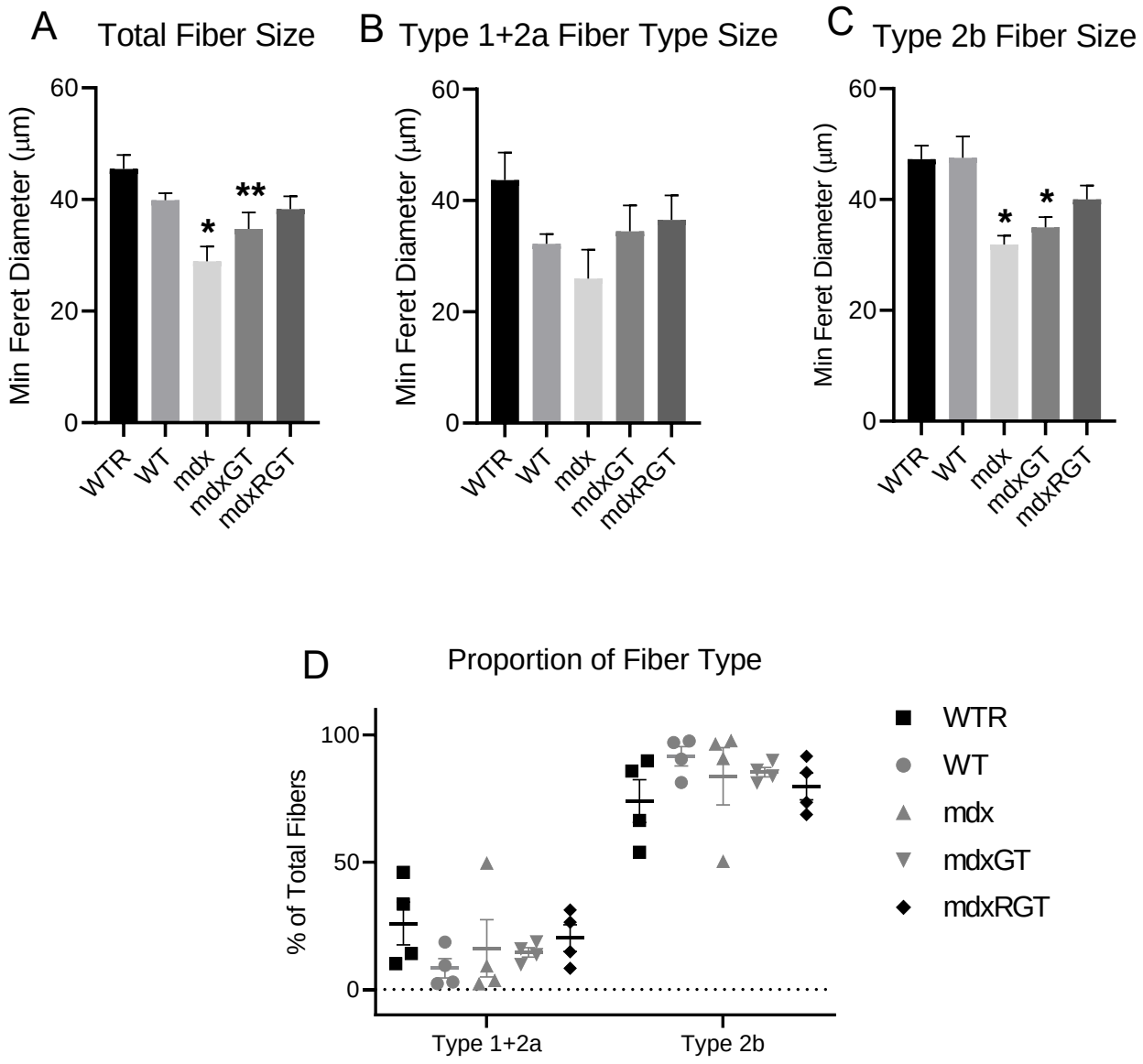

Figure S5. All panels for whole quadriceps. **(A)** Total fiber size, *mdx < WT, WTR; **mdxGT < WTR. **(B, C)** Fiber size by type *mdx, mdxGT < WT, WTR. **(D)** Proportion of fiber type, no differences. All comparisons $p<0.05$. All groups n=4.

Supplemental Tables

Table S1. Revertant fibers in muscles of treated mice as % positivity of Dys2 (Leica).

	mdxGT	mdxRGT
Quad	<1%	2%
	<1%	<1%
	<1%	0
	<1%	<1%
	5%	<1%
	<1%	<1%
	<1%	1%
	<1%	0
Heart	0	0
	0	0
	0	0
	0	0
	0	0
	0	0
	0	0
	0	0
EDL	0	<1%
	0	<1%
	0	<1%
	0	0
	<1%	<1%
	<1%	<1%
	<1%	0
	<1%	0

Table S2. Microdystrophin quantification of MANEX1011b expression in fibers of treated mdx mice as % positivity. Mean ± SE. No differences.

	mdxGT (n=8)	mdxRGT (n=8)
Quad	71.9±6.0	76.3±6.0
Heart	100±0.0	100±0.0
EDL	88.1±3.4	72.5±7.5

Table S3. Western blot quantification of microdystrophin protein in muscles of treated mice, normalized to β-tubulin. *mdxRGT> mdxGT; **mdxGT> mdxRGT. Mean ± SE. All comparisons $p<0.05$.

	mdxGT (n=8)	**mdxRGT (n=8)**
Quad	0.52±0.09	0.85±0.10*
Heart	1.24±0.06	1.18±0.02
Diaphragm	1.14±0.13**	0.84±0.06

Table S4. Treadmill training and fatigue protocols. The fatigue protocol was developed in a preliminary study in the Grange Lab using references cited here.[1–3] Steps 1-6 of the fatigue protocol increase speed linearly from the initial to the final speed; steps 7-11 maintain the same speed over a longer duration.

Training Protocol			**Fatigue Protocol**			
Step	Duration (s)	Speed (m/s)	Step	Duration (s)	Initial Speed (m/s)	Final Speed (m/s)
1	120	0.02	**1**	120	0.02	0.04
2	120	0.04	**2**	120	0.04	0.06
3	120	0.06	**3**	120	0.06	0.08
4	120	0.08	**4**	120	0.08	0.1
5	120	0.1	**5**	120	0.1	0.2
6	120	0.2	**6**	120	0.2	0.3
7	120	0.3	**7**	1200	0.3	0.3
8	120	0.4	**8**	1200	0.35	0.35
9	120	0.5	**9**	1200	0.4	0.4
10	120	0.6	**10**	1200	0.45	0.45
			11	1200	0.5	0.5

Table S5. Treadmill data presented as mean±SE. *WTR > mdx groups; **WTR and mdxRGT > all other groups; $^{\#}$mdx < all other groups; †mdxGT > mdx; ‡mdxRGT > all groups. All comparisons $p<0.05$. WTR, n=7; WT, n=8; mdx, n=7; mdxGT, n=8; mdxRGT, n=8.

	WTR	**WT**	**mdx**	**mdxGT**	**mdxRGT**
Baseline absolute (min)	48.8±12.7*	41.2±8.7	17.0±2.6	19.1±4.0	14.7±0.8
Final absolute (min)	126.2±2.0**	67.0±6.6	24.8±3.6$^{\#}$	70.9±4.0	130.0±0.9**
% Baseline	405.3±113.1	204.1±32.9	156.3±23.1	434.4±60.5†	897.6±42.5‡

Table S6. In vivo plantarflexor torque data presented as mean ± SE. *WTR > mdx, mdxGT, mdxRGT; **WTR > mdx; ***mdxRGT > WTR; †mdxRGT > WTR, WT; ‡WTR> mdx, mdxGT; [a] WTR> mdx, mdxGT. All comparisons $p<0.05$. WTR, n=7; WT, n=8; mdx, n=7; mdxGT, n=8; mdxRGT, n=8.

	WTR	**WT**	**mdx**	**mdxGT**	**mdxRGT**
Baseline 120 Hz absolute (mN*m/g)	0.38±0.05*	0.29±0.02	0.22±0.01	0.22±0.02	0.22±0.01
2 wk post 120 Hz absolute (mN*m/g)	0.35±0.04	0.34±0.04	0.25±0.02	0.34±0.04	0.34±0.03
20 wk post 120 Hz absolute (mN*m/g)	0.41±0.03**	0.35±0.02	0.26±0.01	0.31±0.02	0.34±0.02
2 wk post % Baseline	103.3±21.3	115.4±11.2	116.6±15.1	166.3±27.8	158.1±19.2
4 wk post % Baseline	122.9±10.1	123.2±7.6	127.3±13.5	161.1±13.1	169.2±12.6
8 wk post % Baseline	100.6±13.9	125.6±11.5	109.9±7.3	151.8±17.4	166.1±15.6***
12 wk post % Baseline	116.8±24.9	115.5±9.9	129.6±9.4	155.4±22.3	181.6±16.9†
16 wk post % Baseline	124.7±11.8	121.9±12.2	116.5±7.5	153.4±29.5	167.1±10.9
20 wk post % Baseline	112.7±12.6	125.3±14.0	120.0±11.1	146.8±20.5	157.1±18.3
120 Hz at 2 wk post as % WT	104.5±12.2		74.0±6.9	101.8±12.6	102.1±10.2
120 Hz at 20 wk post as % WT	114.9±8.7‡		72.5±3.2	86.5±5.6	94.8±5.0
20 wk as % 2 wk	122.7±15.2	114.7±15.7	108.5±12.3	99.2±12.8	104.4±11.7
20 wk as % WT 2 wk	120.8±9.1[a]		76.2±3.3	91.0±5.9	99.7±5.2

Table S7. In vivo plantarflexor power data mean ± SE. *WTR> mdxRGT; **WT>mdx, mdxRGT; ***WTR>mdx; [†]WTR > mdx, mdxGT; [††]WT > mdx; [‡]mdxRGT > mdx; [a]mdxRGT > WT; [b]mdxRGT > WTR, WT, mdx; [c]mdxRGT > WT, mdx; [d]WTR > mdx; [e]WTR > mdx, mdxGT; [f]mdxRGT > mdx. All comparisons $p<0.05$. WTR, n=7; WT, n=8; mdx, n=7; mdxGT, n=8; mdxRGT, n=8.

	WTR	**WT**	**mdx**	**mdxGT**	**mdxRGT**
Baseline 40% absolute (mW/g)	1.2±0.3*	1.2±0.2**	0.6±0.1	0.7±0.1	0.6±0.1
2 wk post 40% absolute (mW/g)	1.2±0.1***	0.9±0.1	0.6±0.1	0.9±0.1	0.9±0.1
20 wk post 40% absolute (mW/g)	1.4±0.2[†]	1.1±0.1[††]	0.5±0.1	0.8±0.2	1.1±0.1[‡]
2 wk post % Baseline	68.5±38.6	69.7±24.5	73.3±25.4	153.6±30.9	136.0±43.7
4 wk post % Baseline	116.0±44.2	143.0±54.2	85.3±32.2	170.5±45.7	135.3±54.5
8 wk post % Baseline	105.5±33.8	99.0±26.4	67.3±20.6	151.5±22.5	212.2±42.6
12 wk post % Baseline	165.0±52.3	93.0±34.8	94.8±25.3	111.5±44.7	244.7±62.0[a]
16 wk post % Baseline	123.2±27.4	101.2±15.0	90.5±32.3	151.6±31.0	296.3±62.9[b]
20 wk post % Baseline	152.5±39.9	94.2±44.2	85.0±24.6	123.1±40.2	246.9±58.6[c]
40% Power at 2 wk post as % WT	147.2±10.2[d]		68.5±8.8	104.3±16.1	111.7±11.5
40% Power at 20 wk post as % WT	135.2±18.9[e]		44.2±6.0	77.4±18.7	103.8±9.5[f]

Table S8. In vitro diaphragm and EDL power, force, and stress data; mean ± SE. *WTR, WT > mdx, mdxRGT; **WTR, WT, mdxRGT > mdxGT; ***WTR > mdx, mdxRGT; †WTR > mdx; ††WT > mdx, mdxRGT; ‡WTR > mdx, mdxRGT; ‡‡WTR > mdx. All comparisons $p<0.05$. WTR, n=7; WT, n=8; mdx, n=7; mdxGT, n=8; mdxRGT, n=8.

	WTR	**WT**	**mdx**	**mdxGT**	**mdxRGT**
Diaphragm 40% absolute power	0.18±0.02*	0.17±0.02*	0.07±0.01	0.13±0.02	0.1±0.02
EDL 40% absolute power	1.82±0.16	1.90±0.18	1.46±0.14	1.69±0.18	1.72±0.11
Diaphragm 40% power as % of mdx	267.1±34.9**	250.4±21.8**		192.9±23.6	151.0±23.2**
EDL 40% power as % of mdx	124.6±10.8	129.6±12.5		115.3±12.3	117.8±7.5
Diaphragm 40% power as % of WT	106.7±13.9***		39.9±5.3	77.1±9.4	60.3±9.3
EDL 40% power as % of WT	96.1±8.4		77.1±7.5	88.9±9.5	90.8±5.8
Diaphragm 150 Hz absolute force	15.6±1.1†	17.0±1.0††	9.4±0.5	12.8±1.7	10.5±1.4
EDL 150 Hz absolute stress	319.2±23.0	312.8±27.4	229.6±16.9	266.4±23.0	287.0±17.2
Diaphragm 150 Hz normalized force % WT	91.7±6.2‡		55.1±3.0	75.1±9.9	61.8±8.4
EDL 150 Hz stress % WT	102.1±7.3‡‡		73.4±5.4	85.2±7.4	91.8±5.5

Table S9. Summary of mean relative levels of functional restoration compared to WT or Baseline as indicated. [a]Data from Figure 5; *mdxGT > all groups; **mdxRGT > mdx; [b]Data from Supplemental Table 6; ***WTR > mdx; [c]Data from Supplemental Table 7; [†]WTR > mdx, mdxGT. [††]mdxRGT > mdx; [d]Data from Supplemental Table 8; [‡]WTR > mdx, mdxRGT. [‡‡]WTR > mdx. All comparisons $p < 0.05$. WTR, n=7; WT, n=8; mdx, n=7; mdxGT, n=8; mdxRGT, n=8.

	WTR	**WT**	**mdx**	**mdxGT**	**mdxRGT**
Running wheel distance (% Week 1 distance)[a]	126				194
Final Treadmill time (% of Baseline time)[a]	405	204	156	434*	898**
Final Treadmill time (fold change vs WT)[a]	2.0		0.8	2.1	4.4
Plantarflexor 120 Hz torque at 2 weeks (%WT)[b]	105		74	101	102
Plantarflexor 120 Hz torque at 20 weeks (%WT)[b]	115***		73	87	95
Plantarflexor power at 40% load at 2 weeks (%WT)[c]	147***		69	104	112
Plantarflexor power at 40% load at 20 weeks (%WT)[c]	135[†]		44	77	103[††]
Diaphragm 150 Hz normalized force (%WT)[d]	92[‡]		55	75	62
Diaphragm power at 40% load (%WT)[d]	107[‡]		40	77	60
EDL 150 Hz stress (%WT)[d]	102[‡‡]		73	85	92
EDL power at 40% load (%WT)[d]	96		77	89	91

Table S10. Mitochondrial substrates and corresponding targets.

Substrate	Mitochondrial Target
Malate	Complex I
Pyruvate	Complex I
Glutamate	Complex I
Succinate	Complex II
ADP	Complex V
Cytochrome C	Index of mitochondrial membrane integrity
FCCP (not shown)	Uncouples mitochondrial membrane

Table S11. Mouse morphology. *mdx >WT, WTR, mdxRGT; **mdxGT> WT, WTR; ***WT< mdx, mdxGT, mdxRGT; ****WTR < mdxGT; †WT > mdx, mdxGT, mdxRGT; ††WTR> mdx, mdxGT, mdxRGT; †††mdxGT> mdx; $^{\#}$mdx>WT, WTR; $^{\#\#}$mdxGT>WT, WTR; $^{\#\#\#}$mdxRGT>WT; ‡mdx > WT, WTR; ‡‡mdxGT> WT, WTR. All comparisons $p<0.05$. WTR, n=7; WT, n=8; mdx, n=7; mdxGT, n=8; mdxRGT, n=8.

	WTR	WT	mdx	mdxGT	mdxRGT
Mouse mass at start of study (g)	16.03±2.08	15.61±1.78	16.23±1.63	16.33±1.28	16.43±1.19
Mouse mass at sacrifice (g)	31.04±0.59	31.81±0.61	35.83±0.57*	34.63±0.59**	32.55±0.68
Diaphragm mass (mg)	6.40±0.34****	5.26±0.32***	6.87±0.32	8.04±0.39	7.80±0.44
Diaphragm length (mm)	10.40±0.37††	9.56±0.13†	7.46±0.25	8.45±0.19†††	7.76±0.19
EDL mass (mg)	11.01±0.60	10.60±0.35	15.00±0.87$^{\#}$	13.60±0.14$^{\#\#}$	12.86±0.64$^{\#\#\#}$
EDL length (mm)	10.41±0.14	10.01±0.29	10.59±0.17	10.33±0.22	10.30±0.29
EDL cross sectional area (mm^2)	1.00±0.05	1.00±0.03	1.34±0.08‡	1.25±0.03‡‡	1.18±0.05

Supplemental Methods

Metabolic enzyme assays

Red and white muscle tissue from the left gastrocnemius were separated by careful dissection.[5] The left soleus muscle was combined with the red tissue from the gastrocnemius. White muscle was separated from quadriceps as described in the mitochondrial respiration section. Both red and white muscle portions were assayed for citrate synthase (CS), malate dehydrogenase (MDH), phosphofructokinase (PFK), β-hydroxyacyl-CoA dehydrogenase (βHAD) and cytochrome c oxidase (COX) enzyme activities (all in μmol/mg protein/min). The maximal activities of CS, a biochemical marker of mitochondrial density and oxidative capacity[6,7] and *β*HAD, a key regulatory enzyme in the beta oxidation of fatty acids to acetyl Co A, were determined spectrophotometrically (Biotek Synergy 2 with Gen 5 software, Biotek Instruments, Inc. Winooski, VT) in muscle homogenates as described previously.[8,9]

MDH, a key enzyme in the citric acid cycle and the malate-aspartate shuttle was assayed spectrophotometrically at 340nm at 37°C. Briefly, 10ul of sample were pipetted in triplicate into a clear, flat bottom 96-well plate. Then, 290ul of reaction media (0.1 M potassium phosphate buffer, pH=7.4 plus 0.006 M oxaloacetic acid, prepared in potassium phosphate buffer plus 0.00375 M NADH, was added to the wells and samples were read for 5 minutes at 340nm to determine the maximum rate of disappearance of NADH.

PFK, a rate-limiting step in glycolysis was assayed spectrophotometrically at 340nm by observing the oxidation of NADH to NAD in the presence of fructose 6 phosphate. Briefly, 30ul of sample homogenate were pipetted in triplicate. Then, assay buffer (12 mM MgCl2 , 400 mM KCL, 2 mM AMP, 1 mM ATP, 0.17 mM NADH, 0.0025 mg/mL antimycin, 0.05 mg/mL aldolase, 0.05 mg/mL GAPDH, in 100mM Tris buffer, pH=8.2) was added into each well. After a 2-minute background reading, 3 mM fructose-6-phosphate was added to each sample well followed by a 5 minute kinetic reading to detect maximum changes in absorbance across time.

COX, which transfers electrons between complex III and IV of the electron transport chain was assayed based on the oxidation of ferrocytochrome c to ferricytochrome c by COX. Absorbance was measured at 550nm every 10 seconds for 5 minutes to determine maximum COX activity.

Ex vivo contractile properties

Equipment and software

Ex vivo contractile properties were determined with ASI equipment and software including two 1N dual mode servomotors (300C; ASI) with a lever arm displacement maximum of 10 mm (from +5 to -5 mm), and a 701C High Power Follow Stimulator set to constant voltage. Dynamic Muscle Control (DMC) software controlled the timing and frequency of the stimulations and collection of force (mN) and lever arm displacement (mm). EDL muscles and diaphragm strips were incubated in jacketed water baths (Radnoti, Inc., Covina, CA) that contained an oxygenated (95% O_2–5% CO_2) physiological salt solution (PSS; pH 7.6; in mM): 120.5 NaCl, 4.8 KCl, 1.2 $MgSO_4$, 20.4 $NaHCO_3$, 1.6 $CaCl_2$, 1.2 NaH_2PO_4, 10.0 dextrose, and 1.0 pyruvate. Muscle baths were maintained at 30°C by an HTP-1500 heat therapy pump (Adroit Medical Systems). Dynamic Muscle Analysis (DMA; ASI) was used to analyze the force and displacement data.

Muscle Preparation

EDL

The EDL was carefully dissected and hung between a clamp at the base of the PSS-filled muscle bath and the lever arm of the 300C (4-0 suture), at 10 mN resting tension (Lo; muscle length at which twitch force was maximal) as described.[10]

Diaphragm

The whole diaphragm complete with ribs was laid on a Kim wipe soaked with PSS. A ~4mm wide strip was cut from the costal margin ~3mm lateral to the xyphoid process to the central tendon with a #11 scalpel blade. The attached rib was clamped at the bottom of the muscle bath and tied with 4-0 suture from the central tendon to the lever arm of the 300C.

Pre-contractions

Both the EDL muscles and the diaphragm strips were stimulated to contract via closely flanking platinum wire electrodes ~2mm either side and parallel to the muscle/strip. After 10 min of quiescence, 3 twitches (1 min apart) and 3 tetani at 150 Hz (1 min apart) were

elicited at 30v. Resting tension was reset to 10 mN after each contraction. Hereafter, the muscle/strip resting tension was stable for subsequent assays. Calipers were used to measure muscle/strip length to the nearest 0.1mm.

Force-frequency – Diaphragm and EDL

Following the pre-contractions and after an additional 10 min of rest, the force-frequency relationship was determined at 1, 10, 30, 50, 65, 80, 100, 120, 150, and 180Hz (each for 700 ms duration and each separated by 1 min). Diaphragm contractile responses were expressed as force normalized to strip mass (mN/mg). EDL contractile responses were expressed as stress or force/muscle cross sectional area (CSA; mN/mm2).[11]

Force-velocity and Power - Diaphragm

After 5 min quiescence, the force-velocity relation was determined by the tetanic afterload method. Fractional loads were set at 0.05, 0.10, 0.20, 0.30, 0.40, 0.50, 0.75 and 0.90 of maximum isometric tetanic force (150 Hz). At each load, muscles were stimulated at 150 Hz for 0.5s duration, one minute between each. Data were initially plotted as load in mN vs velocity in mm/s, and the Hill equation was used to fit a curve, generate an equation (Graphpad Prism, GraphPad Software Inc., La Jolla, CA), and to determine Vmax (the maximal velocity of shortening at 0.0 fractional load). Final plots are fractional load of maximum tetanic force vs velocity in mm/s).

Eccentric injury protocol – Diaphragm and EDL

After 5 min quiescence, the eccentric injury protocol was performed.[12] Briefly, muscles were subjected to 5 stretches, each separated by 4 min. For each stretch, both EDL and diaphragm muscles were stimulated at 80 Hz for 700 ms: a 500 ms isometric contraction, followed by a stretch at 0.5 Lo/s for the final 200 ms. This yielded a stretch amplitude of 0.1 Lo. Five min after the last stretch, to assess recovery, an 80Hz isometric contraction was elicited, followed 1 min later by a 150Hz isometric contraction (recovery data not shown).

Diaphragm and EDL morphological characteristics

When all in vitro contractile assays were complete, the sutures and excess tendon were removed from the EDLs, and the suture and rib from the diaphragms, and the muscles/strips lightly blotted. Muscle masses were then determined to the nearest 0.1 mg on an A-200D electronic analytical balance (Denver Instruments, Bohemia, NY).

Statistical analysis

Graphpad Prism 8.0 was used to perform all statistical analyses. Data were analyzed with a one-Way (group) or a two-way ANOVA (e.g., group x time) as required. If a significant interaction between two factors occurred, Tukey's HSD test was used to determine differences between means. Data are presented as mean ± SEM. Statistical significance was accepted at $p \leq 0.05$.

Transcriptome Analysis: RNASEQ Sample Preparation

Muscle samples for transcriptomic analyses were stored in RNALater at - 80°C until analysis. Samples were shipped to and processed by Genewiz (South Plainfield, NJ 07080). RNA samples were quantified using Qubit 2.0 Fluorometer (Invitrogen, Carlsbad, CA, USA) and RNA integrity checked using Agilent TapeStation 4200 (Agilent Technologies, Palo Alto, CA, USA). RNA sequencing libraries were prepared using the NEBNext Ultra RNA Library Prep Kit for Illumina using manufacturer's instructions (NEB, Ipswich, MA, USA). Briefly, mRNAs were initially enriched with Oligod(T) beads. Enriched mRNAs were fragmented for 15 minutes at 94 °C. First strand and second strand cDNA were subsequently synthesized. cDNA fragments were end repaired and adenylated at 3'ends, and universal adapters were ligated to cDNA fragments, followed by index addition and library enrichment by PCR with limited cycles. The sequencing libraries were validated on the Agilent TapeStation (Agilent Technologies, Palo Alto, CA, USA), and quantified using a Qubit 2.0 Fluorometer as well as by quantitative PCR (KAPA Biosystems, Wilmington, MA, USA). Libraries were sequenced using illumina HiSeq platform with the 2x150bp read length configuration. Sequencing reads were trimmed with Trimmomatic v.0.36 and mapped to the *Mus musculus* GRCm38 reference genome using STAR aligner v.2.5.2.b. Gene counts were generated from the resulting BAM files using featureCount from the Subread package v.1.5.2. Count tables from Genewiz were then used to determine relative expression of *Myh* transcripts, as in Terry et al., 2018. [13]

Supplemental References

1. Kregel, K.C., Allen, D.L., Booth, F.W., Fleshner, M.R., Henriksen, E.J., and Musch, T.I. Resource Book for the Design of Animal Exercise Protocols. 152.
2. Aartsma-Rus, A., and van Putten, M. (2014). Assessing Functional Performance in the Mdx Mouse Model. J Vis Exp.
3. Dougherty, J.P., Springer, D.A., and Gershengorn, M.C. (2016). The Treadmill Fatigue Test: A Simple, High-throughput Assay of Fatigue-like Behavior for the Mouse. J Vis Exp.
4. Burns, D.P., Canavan, L., Rowland, J., O'Flaherty, R., Brannock, M., Drummond, S.E., O'Malley, D., Edge, D., and O'Halloran, K.D. (2018). Recovery of respiratory function in mdx mice co-treated with neutralizing interleukin-6 receptor antibodies and urocortin-2. J Physiol *596*, 5175–5197.
5. Bloemberg, D., and Quadrilatero, J. (2012). Rapid Determination of Myosin Heavy Chain Expression in Rat, Mouse, and Human Skeletal Muscle Using Multicolor Immunofluorescence Analysis. PLoS One *7*.
6. Blomstrand, E., Rådegran, G., and Saltin, B. (1997). Maximum rate of oxygen uptake by human skeletal muscle in relation to maximal activities of enzymes in the Krebs cycle. J Physiol *501*, 455–460.
7. Larsen, S., Nielsen, J., Hansen, C.N., Nielsen, L.B., Wibrand, F., Stride, N., Schroder, H.D., Boushel, R., Helge, J.W., Dela, F., et al. (2012). Biomarkers of mitochondrial content in skeletal muscle of healthy young human subjects. J Physiol *590*, 3349–3360.
8. Frisard, M.I., McMillan, R.P., Marchand, J., Wahlberg, K.A., Wu, Y., Voelker, K.A., Heilbronn, L., Haynie, K., Muoio, B., Li, L., et al. (2010). Toll-like receptor 4 modulates skeletal muscle substrate metabolism. Am. J. Physiol. Endocrinol. Metab. *298*, E988-998.
9. Heilbronn, L.K., Civitarese, A.E., Bogacka, I., Smith, S.R., Hulver, M., and Ravussin, E. (2005). Glucose tolerance and skeletal muscle gene expression in response to alternate day fasting. Obes. Res. *13*, 574–581.
10. Wolff, A.V., Niday, A.K., Voelker, K.A., Call, J.A., Evans, N.P., Granata, K.P., and Grange, R.W. (2006). Passive mechanical properties of maturing extensor digitorum longus are not affected by lack of dystrophin. Muscle Nerve *34*, 304–312.
11. Sperringer, J.E., and Grange, R.W. (2016). In Vitro Assays to Determine Skeletal Muscle Physiologic Function. Methods Mol Biol *1460*, 271–291.
12. Petrof, B.J., Shrager, J.B., Stedman, H.H., Kelly, A.M., and Sweeney, H.L. (1993). Dystrophin protects the sarcolemma from stresses developed during muscle contraction. Proc Natl Acad Sci U S A *90*, 3710–3714.
13. Terry, E.E., Zhang, X., Hoffmann, C., Hughes, L.D., Lewis, S.A., Li, J., Wallace, M.J., Riley, L.A., Douglas, C.M., Gutierrez-Monreal, M.A., et al. (2018). Transcriptional profiling reveals extraordinary diversity among skeletal muscle tissues. eLife *7*, e34613.